

Crack Coalescence in Rock Bridges under Uniaxial Compression

단축압축 하의 암석 브릿지에서의 균열 결합



박남수*¹
Park, Nam-Su



전석원*²
Jeon, Seokwon

Abstract

Rock masses are usually discontinuous in nature, as a result of various geological processes they have undergone and they contain rock joints and bridges. Crack propagation and coalescence processes mainly cause rock failures in tunnels. In this study, we focused on the crack initiation, propagation and coalescence process of rock materials containing two pre-existing open cracks arranged in different geometries. During uniaxial compression, wing crack initiation stress, wing crack propagation angle, and crack coalescence stress of Diastone gypsum and Yeosan Marble specimens were examined. And crack initiation, propagation, and coalescence processes were observed. Shear, tensile and mixed (shear+tensile) types of crack coalescence occurred. To compare the experimental results with Ashby & Hallam model, crack coalescence stress was normalized and it generally agreed with the experimental results.

Keywords : Rock bridges, Wing crack, Crack coalescence, Ashby & Hallam model

*¹ 서울대학교 지구환경시스템공학부

*² 정회원, 서울대학교 지구환경시스템공학부 조교수

요 지

암석은 지질학적 생성과정으로 인해 많은 역학적 결함을 포함하고 있으며 이러한 결함 사이에는 암석 브릿지가 존재하게 된다. 이러한 암석 브릿지에서의 균열의 전파 및 결합(coalescence)과정은 터널의 안정성에 영향을 미치게 된다. 본 연구에서는 단축압축 하에서 균열의 형상변화에 따른 암석 브릿지에서의 균열의 개시, 전파 및 결합거동 변화를 강화석고의 일종인 Diastone과 여산 대리석 시료에 대해 알아보았다. 하중을 가하면서 날개형 균열 개시응력, 날개형 균열 전파각도, 균열결합 응력을 측정하였으며, 전단, 인장, 혼합형의 3가지 균열결합 유형이 나타났다. 또한, 정규화된 최대강도(normalized peak strength)를 구하여 Ashby & Hallam 모형(1986)의 이론해와 비교, 분석하였다.

주요어 : 암석 브릿지, 날개형 균열, 균열결합, Ashby & Hallam 모형

1. Introduction

Rock masses are usually different from other engineering materials because they contain discontinuities. With such discontinuities, rock masses contain rock bridges, a non-cracked area between pre-existing cracks. Under various types of loading, cracks start to grow from pre-existing cracks, propagate, and coalesce with neighboring cracks in rock bridges. These processes mainly cause rock failures in rock structures such as tunnels.

Crack initiation and propagation have been one of the most intensive subjects in rock mechanics and a number of researches have been done on crack propagation in different materials in uniaxial compression (Nemat-Nasser & Horii, 1982; Hoek & Bieniawski, 1984; Jiefan et al., 1990).

But these researches were mainly focused on the crack initiation, propagation, and researchers on the crack coalescence in rock bridges have started recently. With some experimental results of crack behavior under shear loading (Li et al., 1990), both experimental and numerical researches on crack coalescence in rock bridges under uniaxial

compression have been reported (Reyes & Einstein, 1991; Shen, 1995; Wong & Chau, 1998; Bobet & Einstein, 1998). However, most experimental studies conducted on a limited test material and pre-existing crack arrangement.

In this study, we focused on the crack initiation, propagation and coalescence process of rock materials containing two pre-existing open cracks arranged in different geometries. Specimens of 120 60×25 mm in size were prepared. They were made of Diastone gypsum and Yeosan Marble. In the specimens, two artificial cracks were cut with pre-existing crack angle α , bridge angle $\hat{\alpha}$, pre-existing crack length $2c$, and bridge length $2b$. Wing crack initiation stress, wing crack propagation angle, and crack coalescence stress were measured, and crack initiation, propagation, and coalescence processes were observed during uniaxial loading at the loading rate of 0.003 kN/s. Crack coalescence stress was normalized to compare the experimental results with Ashby & Hallam model (1986).

2. Experimental Study

Table 1. Physical and mechanical properties of test materials

Properties	Specimen	Diastone	Yeosan Marble
Bulk specific gravity		1.86	2.71
Apparent porosity (%)		0.10	0.26
P-wave velocity (m/sec)		3,470	3,210
S-wave velocity (m/sec)		1,760	1,710
Uniaxial compressive strength (MPa)		33	57
Young's modulus (GPa)		11.6	39.3
Poisson's ratio		0.23	0.29
Brazilian tensile strength (MPa)		3.0	5.0
Fracture toughness, KIC (MPa√m)		0.6931	1.2847

2.1 Test Materials

To compare the results of rock and rock-like material, we used Diastone gypsum and Yeosan Marble as test materials. The physical and mechanical properties of test materials are summarized in Table 1. Diastone gypsum is a mixture of Diastone (Diastone MR-150) and water at the weight ratio of Diastone to water 100: 26. In Diastone specimen, pre-existing cracks were notched by inserting two 0.3 mm thick steel plates. Specimens were cured at room temperature for 1 day followed by in an oven at 105°C for another day. To make a pre-existing crack in marble specimen, a 3 mm diameter starter hole was drilled and pre-existing cracks were notched by 0.3 mm thick diamond wire saw.

2.2 Specimen Geometries

The dimension of the specimens was 60×120×25 mm. Two pre-existing crack were created in the width of 0.3mm. The positions and orientations of pre-existing cracks were determined by varying

pre-existing crack angle, bridge angle, pre-existing crack length 2c, and bridge length 2b. Pre-existing crack angle varied from 30° to 75° with 15° increments and bridge angle was angled at 45°, 60°, 90°, 120°, 135° and 150° to examine the effect of non-overlapping cracks ($\beta < 90^\circ$) and overlapping cracks ($\beta \geq 90^\circ$). Pre-existing crack length and bridge length varied with 10, 15 and 20 mm.

When pre-existing crack length and bridge length were 10mm, all pre-existing crack angle and bridge angle was tested. To study the effect of pre-existing crack length and bridge length on the process of crack coalescence and peak strength, pre-existing crack length and bridge length were fixed at 10 mm and bridge length and pre-existing crack length were changed into 15 and 20 mm. In this case, pre-existing crack angle or bridge angle was fixed at 45°. Specimens are numbered in the order of a serial number, material, pre-existing crack angle, and bridge angle. For example, D713 means Diastone specimen of which the pre-existing crack length and bridge length is 10 mm, pre-existing crack angle is 75°, and bridge angle is

Table 2. Specimen numbers
(D: Diastone gypsum, M: Marble)

Specimen		Pre-existing crack length (2c, mm)	Bridge length (2b, mm)
D	M	10	10
1D	1M	10	15
2D	2M	10	20
3D	3M	15	10
4D	4M	20	10

135°. Specimen numbers are listed in Table 2.

The uniaxial compression tests were performed in SHIMADZU UDH-200AR loading machine at the loading rate of 0.003 kN/s. All specimens were loaded until either crack coalescence occurred or specimen failed. Load and displacement data were measured with LVDT and recorded through Measurement Groups System 5000 data acquisition system. During tests, crack initiation, propagation, and coalescence were observed through a

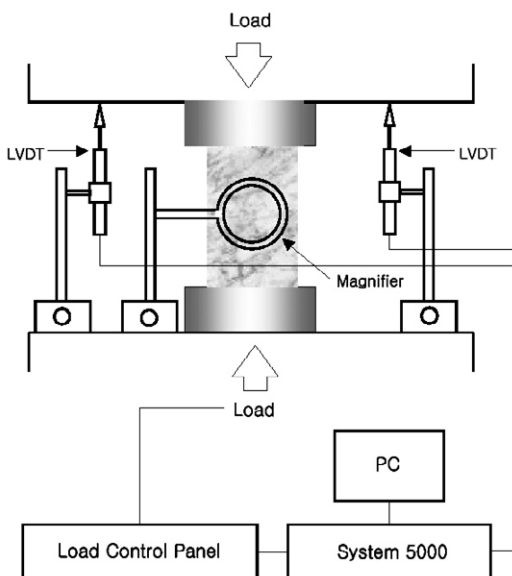


Fig. 1 Schematic diagram of test setup

magnifier, and wing crack initiation stress, wing crack propagation angle, and crack coalescence stress were measured. A schematic diagram of test setup is shown in Fig. 1.

3. Ashby & Hallam Model

To explain the non-linear stress-strain behavior of rock under uniaxial compression, a number of numerical models have been studied and among them a sliding crack model has been successfully used (Kemeny 1987, Jeon & Shin 1999). Frictional cracks of angle α with length $2c$ under uniaxial compression are considered in sliding crack model as shown in Fig. 2.

Ashby & Hallam (1986) derived the following equation for the mode I stress intensity factor K_I at

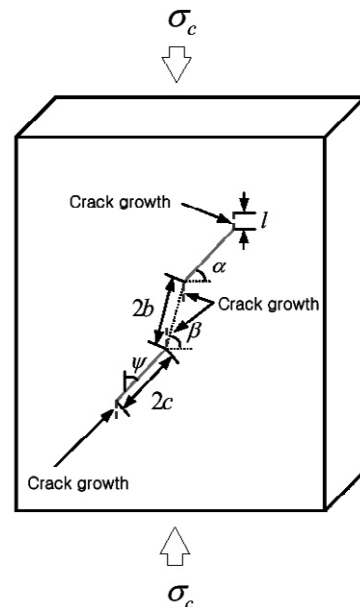


Fig. 2 Model containing two neighboring preexisting cracks of length $2c$

the tip of pre-existing cracks from compression test of PMMA materials using sliding crack model,

$$\frac{K_I}{\sigma_c \sqrt{\pi c}} = \frac{\sin 2\psi - \mu + \mu \cos 2\psi}{(1 + L)^{3/2}} \left[0.23 L + \frac{1}{\sqrt{3(1 + L)}} \right] \quad (1)$$

where, $\psi = 90 - \alpha$; μ = frictional coefficient; $L = l/c$, normalized wing crack length,

Stress intensity factor due to crack interactions using beam theory can be derived as follows,

$$\frac{K_I}{\sigma_c \sqrt{\pi c}} = \left[\frac{2 \varepsilon_0 (L + \cos \psi)}{\pi} \right]^{1/2} \quad (2)$$

where, $\varepsilon_0 = c^2 N / A$, crack density (N = number of cracks; A = area of specimen),

Combining Equation (1) and (2) gives the following total stress intensity factor,

$$\frac{K_I}{\sigma_c \sqrt{\pi c}} = \frac{\sin 2\psi - \mu + \mu \cos 2\psi}{(1 + L)^{3/2}} \left[0.23 L + \frac{1}{\sqrt{3(1 + L)}} \right] + \left[\frac{2 \varepsilon_0 (L + \cos \psi)}{\pi} \right]^{1/2} \quad (3)$$

In this study, we assumed the peak strength for rock failure as crack coalescence stress. When crack coalescence occurs, the maximum wing crack length is $l_{\max} = 2b \sin \beta$ and the peak uniaxial compressive strength σ_c^{\max} can be induced by inserting $K_I = K_{IC}$ and $L = L_{cr} = l_{\max} / c$ into Equation (3). The normalized peak strength can be derived as follows,

$$\frac{\sigma_c^{\max} \sqrt{\pi c}}{K_{IC}} = \left\{ \frac{\sin 2\psi - \mu + \mu \cos 2\psi}{(1 + L_{cr})^{3/2}} \left[0.23 L_{cr} + \frac{1}{\sqrt{3(1 + L_{cr})}} \right] + \left[\frac{2 \varepsilon_0 (L_{cr} + \cos \psi)}{\pi} \right]^{1/2} \right\}^{-1} \quad (4)$$

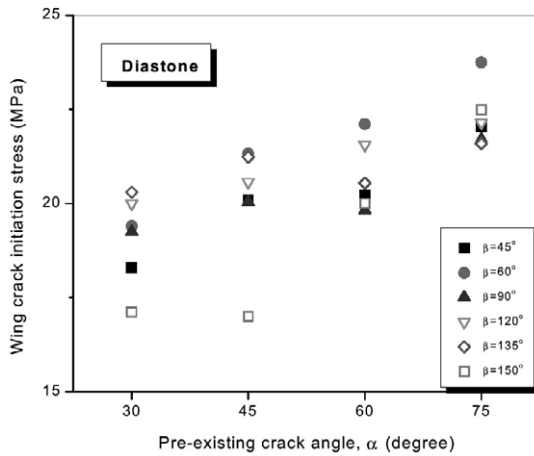
4. Results

4.1 Wing Crack

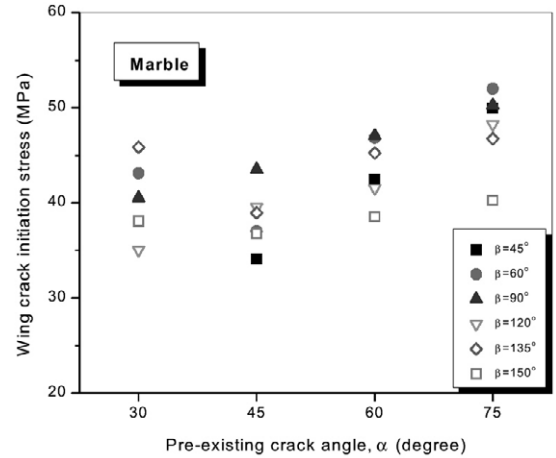
When the load is increased, wing cracks are initiated from the tips of pre-existing crack. Wing cracks are tensile crack and propagate in a curvilinear path as the load is increased. In this study, we measured wing crack initiation stress and wing crack propagation angle.

The relationship between wing crack initiation stress and pre-existing crack angle is plotted in Fig. 3. Wing crack initiation stress was increased with the increase of pre-existing crack angle.

Wing cracks initiate when the maximum tensile stress around the tips of pre-existing crack reaches a critical value and the maximum tensile stress is increased with the increase of pre-existing crack angle. High tensile stress exists around the tips of pre-existing crack, but it decreases away rapidly from the tips with increasing pre-existing crack angle. Therefore, to propagate wing crack and make it visible, greater stress is needed with increasing pre-existing crack angle. This result is coincident with the result of Reyes (1991) and Vasarhelyi & Bobet (2000).



(a) Diastone



(b) Marble

Fig. 3 Pre-existing crack angle vs. wing crack initiation stress

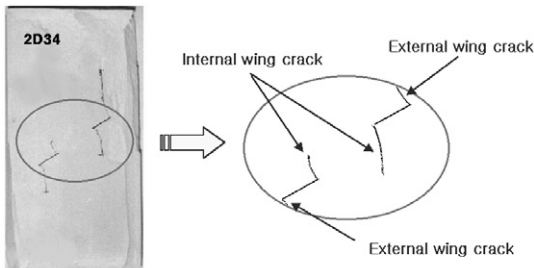


Fig. 4 No occurrence of crack coalescence

4.2 Crack Coalescence

4.2.1 Classification of Crack Coalescence Type

In this study, three types of crack coalescence were observed. Type I was shear cracking, Type II was tensile cracking, which was later divided into

five different sub-types, and Type III was mixed type of shear and tensile cracking. These types of crack coalescence are summarized in Table 3.

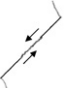






Crack coalescence type depended on bridge angle; In non-overlapping cracks ($\beta < 90^\circ$), Type I crack coalescence occurred and Type II and III crack coalescences occurred in overlapping cracks ($\beta \geq 90^\circ$).

1) Type I: Shear cracking

In this case, wing crack initiated at the inner and outer tips of pre-existing crack first. But shear crack initiated from the inner tips of pre-existing crack and crack coalescence resulted from this shear crack before wing cracks propagate further.

2) Type II: Tensile cracking

Table 3. Classification for three types of crack coalescence

Type	Schematic path of coalescence	Description	Bridge angle	Mode of coalescence
I		Crack coalescence occurred by shear crack	$\beta < 90^\circ$	Shear
II-1		Wing crack initiated from the inner tips of pre-existing crack and coalescence occurred by its propagation	$\beta = 90^\circ$	Tension
II-2		Crack coalescence occurred by tension crack which initiated in the middle of rock bridge during the wing crack propagated	$\beta = 90^\circ$	Tension
II-3		Wing crack initiated from the inner tips of pre-existing crack and coalescence occurred by wing crack in the middle of pre-existing crack	$\beta > 90^\circ$	Tension
II-4		Wing crack initiated from the inner tips of pre-existing crack and coalescence occurred by wing crack in the outer tips of pre-existing crack	$\beta > 90^\circ$	Tension
II-5		Crack coalescence occurred by tension crack which initiated in the middle of rock bridge during the wing crack propagated	$\beta > 90^\circ$	Tension
III		Wing crack initiated from the inner tips of pre-existing crack and coalescence occurred by shear crack which propagated from the wing crack	-	Shear + Tension

Wing crack initiated from the inner tips of pre-existing crack and coalescence occurred by its propagation. Wing crack coalescence can be divided into five sub-types as shown in Table 3. In Diastone specimens, Type II-5 did not occur, but Type II-2 did not occur in Marble specimens.

3) Type III: Mixed (shear + tensile) cracking

Type III coalescence occurred only in Diastone specimens, D713 and 2D49. In this case, wing crack initiated from the inner tips of pre-existing crack, but crack coalescence occurred by shear crack, which propagated from the wing crack.

4.2.2 No Crack Coalescence

As shown in Fig. 4, when the bridge length lied between 1.5 and 2 times of pre-existing crack length, crack coalescence did not occur. This was found for all cases of Diastone specimens but only for non-overlapping cracks of marble specimens.

4.3 Crack Coalescence Stress

In this study, crack coalescence stress are measured to examine how the change of pre-existing crack geometry and test materials affects the strength of rock. To compare the experimental

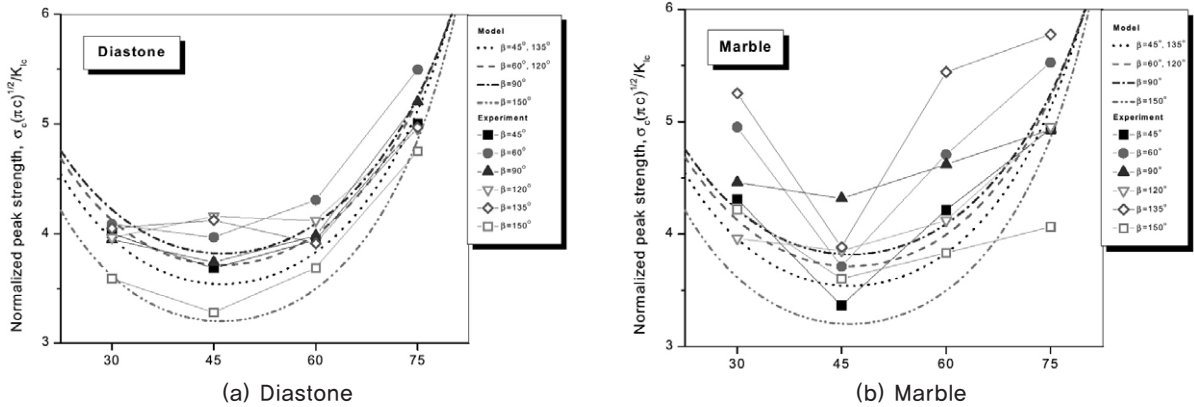


Fig. 5 Pre-existing crack angle vs. normalized peak strength

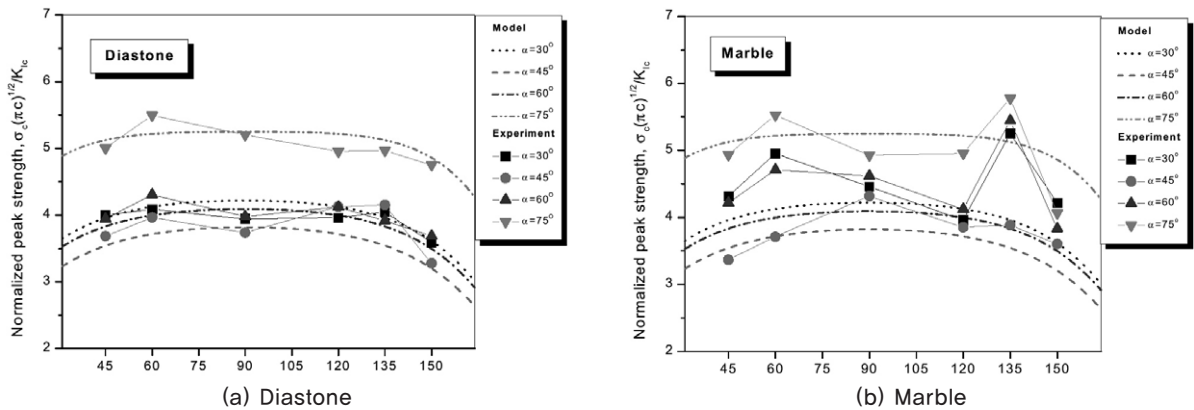


Fig. 6 Bridge angle vs. normalized peak strength

results with Ashby & Hallam model (1986), crack coalescence stress was normalized to normalized peak strength using Equation (4).

4.3.1 The effect of pre-existing angle and bridge angle

The relationship between pre-existing crack angle and normalized peak strength is plotted in Fig. 5 and bridge angle vs. normalized peak strength is plotted in Fig. 6. The solid lines with

symbols are the test results of this study while the dotted lines are analytical prediction using Ashby & Hallam model.

The experimental results generally agreed with the model and the results from Diastone specimens were more coincident with the model than those of marble specimens. The plot of normalized peak strength had a parabolic shape with the minimal at $\alpha=45^\circ$ and the variation of the normalized peak strength had less dependency on bridge angle than

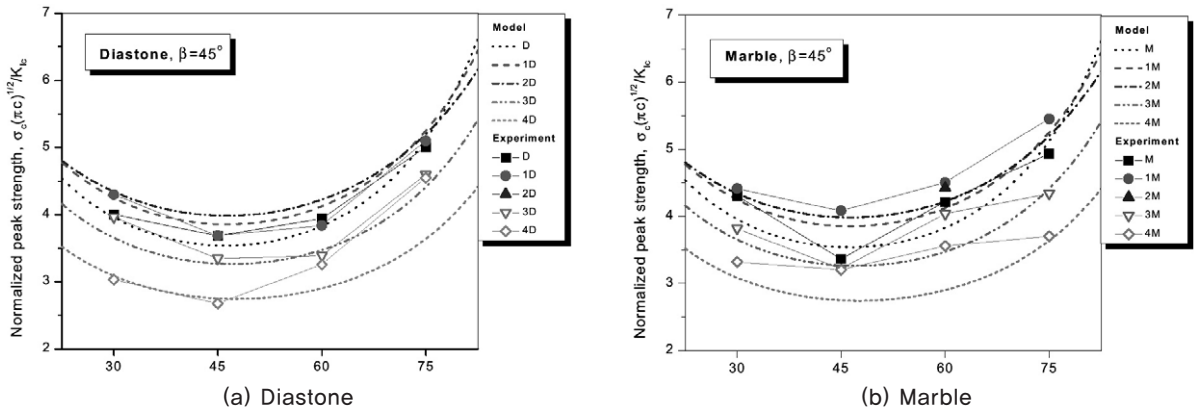


Fig. 7 Pre-existing crack angle vs. normalized peak strength
(when pre-existing crack and bridge length are varied, $\beta=45^\circ$)

pre-existing crack angle.

As shown in Fig. 7, when the bridge length increased, the normalized peak strength increased. Because tensile stress in rock bridge decreased with the increase of bridge length. But the normalized peak strength decreased with the increase of the pre-existing crack length, because the effect of specimen boundaries increased.

5. Conclusions

In this study, we investigated the crack coalescence mechanism of rock materials containing two pre-existing cracks under uniaxial compression, and the effect of pre-existing crack geometries and test materials on crack coalescence mechanism.

Wing crack initiation stress was increased with the increase of pre-existing crack angle. Three types of crack coalescence occurred; Type I was shear cracking, Type II was tensile cracking, which

was later divided into five different sub-types, and Type III was a mixture of shear and tensile cracking. Classification by the types of crack coalescence depended on bridge angle. When the bridge length lies between 1.5 and 2 times of crack length, crack coalescence did not occur. This was found for all cases of Diastone but only for non-overlapping cracks of marble. Crack coalescence stress was normalized to compare with the experimental results with Ashby & Hallam model (1986). The experimental results generally agreed with the model. The plot of normalized peak strength had a parabolic shape with the minimal at $\alpha=45^\circ$ and the variation of the normalized peak strength had less dependency on bridge length than pre-existing crack length. When the bridge length increased, the normalized peak strength increased. While the normalized peak strength decreased with the increase of the pre-existing crack length.

REFERENCE

1. Ashby, M.F. and Hallam, S.D.(1986), "The failure of brittle solids containing small cracks under compressive stress states", *Acta Metall.*, Vol.34, No.3, pp.497-510.
2. Bobet, A. and Einstein, H.H.(1998), "Fracture coalescence in rock-type materials.", *Int. J. Rock Mech. Min. Sci. & Geomech. Abstr.*, Vol.35, No.7, pp.863-888.
3. Hoek, E. and Bieniawski, Z.T.(1984), "Brittle fracture propagation in rock under compression." *Int. J. Frac.*, Vol.26, pp.276-294.
4. Jeon, S. and Shin, J.(1999), "Changes of effective elastic moduli due to crack growth." *Proc. 9th Int. Cong. Rock Mech.*, Vol.2, pp913-915.
5. Jiefan, H., Ganglin, C., Yonghong, Z. and Ren, W.(1990), "An experimental study of the strain field development prior to failure of a marble plate under compression.", *Tectonophysics*, Vol.175, No.6, pp.269-284.
Kemeny, J.M. and Cook, N.G.W.(1987), "Crack models for the failure of rock under compression.", *Proc. 2nd Int. Conf. Constitutive Laws for Eng. Materials*, Vol.2, pp.879-887.
6. Li, C., Stephansson, O. and Savilahti, T.(1990), "Behaviour of rock joints and rock bridges in shear testing.", *Rock Joints, Proc. Int. Symp. Rock Joints*, pp.259-266.
7. Nemat-Nasser, S. and Horii, H.(1982), "Compression-induced nonplanar crack extension with application to splitting, exfoliation and rockburst.", *J. Geophys. Res.*, Vol.87, No.B8, pp.6805-6821.
8. Reyes, O.(1991), "Experimental study and analytical modeling of compressive fracture in brittle materials.", Ph.D. thesis, Mass. Inst. of Technol, Cambridge.
9. Reyes, O. and Einstein, H.H.(1991), Failure mechanism of fractured rock - A fracture coalescence model.", *Proc. 7th Int. Cong. Rock Mech.*, Vol.1, pp.333-340.
10. Shen, B.(1995), "The mechanism of fracture coalescence in compression - experimental study and numerical simulation.", *Eng. Frac. Mech.*, Vol.51, No.1, pp.73-85.
11. Vasarhelyi, B. and Bobet, A.(2000), "Modeling of crack initiation, propagation and coalescence in uniaxial compression.", *Rock Mech. and Rock Eng.*, Vol.33, No.2, pp.119-139.
12. Wong, R.H.C. and Chau, K.T.(1998), "Crack coalescence in a rock-like material containing two cracks.", *Int. J. Rock Mech. Min. Sci. & Geomech. Abstr.*, Vol.35, No.2, pp.147-164.